

523-32
185883
August 15, 1993
P-25
N 94-14392

GOPEX at the Starfire Optical Range

R. Q. Fugate

Starfire Optical Range, Phillips Laboratory, Kirtland Air Force Base, New Mexico

The Starfire Optical Range successfully conducted laser uplink experiments to the Galileo spacecraft during the early morning hours of December 9, 10, 11, and 12, 1992, when the spacecraft was at ranges between 700,000 and 3 million km from Earth. Analysts at JPL have reported as many as 79 pulse detections by the spacecraft. The best weather conditions occurred on the second night when 37 pulses were detected with as many as five on one frame. Signal levels at the spacecraft generally agree with predictions.

I. Introduction

This article summarizes the experiment requirements, design, operations, and results obtained in the Galileo Optical Experiment (GOPEX)[1], conducted by the U.S. Air Force Phillips Laboratory at the Starfire Optical Range (SOR) near Albuquerque, New Mexico. SOR was chosen by JPL, the sponsoring agency, as a second site to complement their operations at Table Mountain Facility (TMF), in Wrightwood, near Los Angeles, California, and to provide geographic diversity, increasing the probability of success in case of bad weather.

The primary objective of GOPEX was to demonstrate that a narrow laser beam pointed at the Galileo spacecraft as it receded from Earth could be detected by the on-board Solid-State Imaging (SSI) camera. This objective was indeed achieved at ranges of approximately 700,000 to six million km from Earth. SOR successfully illuminated the spacecraft on the first four nights of the test, but unfortunately bad weather at the site halted the experiment on

the last three nights. Site diversity proved to be advantageous in the experiment, since TMF was weathered out on the fourth night. A secondary objective was to measure the level and fluctuation in the laser irradiance at the spacecraft and compare the results with theoretical predictions. In general, this objective was also met with a high degree of success.

II. Experiment Requirements

The TMF and SOR sites were each required to transmit bursts of laser pulses on a preset schedule. Each burst lasted approximately three seconds and was computed to start so that pulses arrived at the spacecraft centered about the camera's shutter opening. Individual laser pulses were synchronized within one millisecond of WWV time. Spacecraft-camera shutter-opening times varied from 133-800 msec on a preprogrammed schedule that operated from the internal clock, which was also synchronized with WWV time. The camera was programmed

to scan along a path parallel to the Earth's terminator to spatially separate individual laser pulses on the focal plane. TMF and SOR never operated at the same laser pulse rate, making it possible to uniquely determine each site by measuring the pixel spacing between laser pulse detections.

Uplink operations occurred just before dawn on December 9, 10, 11, 12, 14, 15, and 16, 1992. The uplink times put the SOR very close to the terminator. Table 1 lists for each experiment day the start and end times, the number of transmissions, and the time between transmissions. At a pulse rate of 10 pulses per second, 4710 pulses in total were scheduled to be transmitted toward the Galileo spacecraft from SOR.

The GOPEX Task Manager required that certain diagnostic information be recorded during the uplink transmissions. This information included the energy and pulse width of every laser pulse; the time, to the nearest millisecond, of every laser pulse transmitted; the telescope coordinates during every pulse transmitted; the position of the steering mirror (explained below); and the coherence diameter (Fried's parameter r_0) of the atmosphere. The laser beam divergence at SOR was required to be 80 μrad full-angle during the first four nights and 40 μrad during the last three nights. SOR was required to develop an experimental technique for setting the full-angle beam divergence to better than ± 10 percent.

Navigational data for the spacecraft were given to SOR by JPL in terms of J2000 geocentric state vectors (position, velocity, and acceleration) and mean-of-date pointing predictions for SOR. The state vector data were converted to mean-of-date local mount coordinates by algorithms developed at SOR, and results were compared with JPL pointing predictions. In general, agreement was better than 2 μrad . Consequently, the SOR algorithms were used to point the telescope since they continuously updated the mount pointing. The mount model was validated and occasionally updated by centering the image of a nearby guide star in the field of a CCD camera between propagations. SOR was required to develop a technique to boresight the laser to the CCD guide-star camera to within 5 μrad . SOR was also required to demonstrate these capabilities during precursor tests using high-altitude Earth-orbiting artificial satellites during a dry run.

III. Description of Experiment Hardware

A. General Layout

Figure 1 shows the overall arrangement of the experimental setup at SOR. The laser-transmitting aperture is

a 1.5-m (60-in.) Cassegrain telescope with a coudé path, mounted on elevation-over-azimuth gimbals set on an 8-m-tall hollow pier. The laser and tracking sensors are located in the coudé room on the ground floor of the facility. Three fiber-optic source simulators, located in the pier, are used to set the two values of the laser beam divergence and to represent a star at infinity. The source simulators can be moved into and out of the optical beam path to an angular accuracy of approximately 0.5 μrad , as measured in the output space of the telescope.

B. Telescope and Optics

The 1.5-m telescope is a classical Cassegrain with a parabolic primary mirror and a hyperbolic secondary mirror. The primary mirror has a focal length of 2.2882 m. It is coated with aluminum and a protective silicon monoxide overcoat. The secondary mirror has a focal length of -0.1486 m and a conic constant of -1.028072. The output of the telescope is an f/217 beam, approximately 10 cm in diameter (an angular magnification of ~ 15). The secondary mirror and all coudé mirrors are coated with Denton Vacuum enhanced silver FSS-99 coating.

Light from the telescope (or a laser beam projected by the telescope) is relayed through a coudé path in the center of the pier to the optics room, which is located on the first floor of the facility. Since the telescope is normally used with adaptive optics, the relay optics reimaging the primary mirror of the telescope onto a deformable mirror located on the optics table in the coudé room. No adaptive optics were used in this experiment and the deformable mirror was kept in a "system-flat" mode which removed systematic optical aberrations (approximately 1/10 wave) in the system. Figure 2 shows the coudé path optics and M8, the first element in the imaging relay, a spherical mirror having a focal length of 6.21 m used at a 3.2-deg angle of incidence. This figure also shows the image plane for objects at infinity and the locations of the movable source simulators. Two of the simulators were used to set the beam divergence of the laser to either 80 or 40 μrad , as described later. The simulator representing a source at infinity is at a location along the coudé path that produces the minimum wavefront curvature at the output of the wavefront sensor, as compared with a reference wavefront source located on the optics table. By definition, this sets the location of the infinity source simulator. During telescope operations, the secondary mirror position of the telescope is adjusted (while observing a star) to minimize wavefront curvature as reported by the wavefront sensor.

Figure 3 is a schematic diagram showing the layout of components on the optics table in the coudé room. The

diverging beam from the pier is recollimated by an 8.45-m focal length off-axis parabolic mirror, OAP#1. The beam then reflects from a fast-steering mirror onto the deformable mirror (which is preset with a static figure to remove small residual aberrations in the system). An 11.2-cm diameter image of the telescope's primary mirror is formed on the deformable mirror. Another off-axis paraboloid, OAP#2, and a lens reimaging the deformable mirror on an array of lenslets in the Shack-Hartmann sensor. This sensor is used to set the 1.5-m telescope focus by observing a bright star just prior to operations.

The pulsed laser beam is injected into the coudé path by means of a thin-film plate polarizer located between OAP#2 and the recollimating lens. The total optical transmission from the output of the laser to the atmosphere is estimated to be 43 ± 3 percent. Just prior to laser propagation, the telescope is pointed to a nearby guide star. Light from the guide star passes through the laser-aperture sharing element and is imaged onto a low-noise, high-resolution CCD camera to verify telescope pointing. This camera is the primary sensor for laser boresighting and telescope pointing.

The reference source for the wavefront sensor is placed at the focus of OAP#2, since this point is optically conjugate to infinity. The laser-aperture sharing element is located in the converging beam ahead of the infinity focus. Since the thin-film plate polarizer is used in a converging beam, a glass plate was placed behind it to compensate for the astigmatism in images of the guide star at the CCD camera and during telescope defocus measurements made with the wavefront sensor.

The fast-steering mirror was used to offset the laser pointing direction in a predetermined pattern to increase the probability of detection in the event that the navigation data were in error. The mirror was repositioned between laser pulses to generate either a hexagonal or square pattern, as shown in Fig. 4. These scan patterns were used only on the first night of operations. The scan patterns put the nominal position of the spacecraft in the edge of the beam.

C. Optical Alignment

The basic optical alignment requirements for GOPEX were to (1) establish the optical axis of the system, (2) set the full-angle laser beam divergence to either 80 or 40 μrad , and (3) accurately boresight the laser to the optical axis of the system.

The optical axis of the system was defined in tilt by the CCD guide-star camera and in translation by the cen-

ter of the entrance pupil of the telescope. The required laser beam divergence was generated by focusing the 1.5-m-diameter beam in the atmosphere at ranges of 18.75 and 37.5 km, respectively. These ranges can be simulated at the appropriate conjugate points in the path of the relay-imaging optics in the pier. Based on the optical design of the relay optics, these points are 64.14 cm and 32.703 cm below the location of the infinity focus where a fiber-optic star simulator is located on a stepper motor-driven stage. The laser beam will come to focus at these points in the coudé path when the divergence is properly adjusted. Furthermore, a source accurately positioned at these points is a fiducial for boresighting the laser to objects at infinity imaged on the optical axis of the telescope. Two 50- μm -diameter optical fibers were placed on precision slide stages at these points. The arrangement of the source simulators is shown in Fig. 5. Light transmitted by the fiber was imaged by the CCD guide-star camera and allowed positioning of the stages to approximately 0.5 μrad in the output space of the telescope. The vertical position of the fiber was measured mechanically with an uncertainty of ± 5 mm.

Beam divergence was set by using a knife-edge test on the focused beam and observing the pattern in the plane of the fiber. This technique produces no more than ± 0.5 wave of focus error. The telescope focus error is less than ± 0.25 wave, including higher order aberrations in the optical system between the star simulator and the telescope exit. Assuming worst-case additive errors, the divergence error is $\pm 2.8 \mu\text{rad}$ or 6 percent at 40 and 3 percent at 80 μrad full-angle beam divergence. Final beam boresighting was set by maximizing the light injected into the fiber from the focused laser beam. Beam motion of $\pm 0.5 \mu\text{rad}$ completely extinguishes laser light coming out of the fiber. It was estimated that all error sources would make the worst-case boresight error $\pm 1.75 \mu\text{rad}$ for the 40- μrad beam-divergence case and $\pm 2.25 \mu\text{rad}$ for the 80- μrad beam-divergence case. The actual beam divergence was verified by scanning the beam across high-altitude Earth-orbiting satellites equipped with retro-reflectors.

D. Laser Characteristics

The laser used for these experiments was a frequency-doubled neodymium:yttrium-aluminum-garnet (Nd:Yag), Spectra-Physics Quanta-Ray DCR-2A, field-modified to the equivalent of a DCR-3G. The laser was equipped with Spectra-Physics' unstable Gaussian Coupled Resonator using Radially Variable Reflectivity coatings. This resonator produces a beam profile shaped more like a "top hat" than gaussian. This feature makes it easier to relay

through the optics and produces a more uniform intensity pattern at long ranges. The measured intensity profile in a plane equivalent to approximately 700,000 km is shown in Fig. 6. The laser pulse width was 14.5 nsec (full-width half-maximum), and the energy per pulse was 318 ± 10 mJ per pulse.

E. Telescope Pointing

The two-axis mount of the 1.5-m telescope is controlled by a microcomputer that is designed to accept data on an object's position from imaging cameras or a track processor. The microcomputer is equipped with relatively simple, but very effective, algorithms that compute angular positions and rates of low and high Earth-orbiting artificial satellites, as well as astronomical objects. The computer code is able to modify in real time the orbital parameters of satellites based on measurements of the satellite's position by imaging cameras or trackers.

The routines for pointing the telescope at a selected guide star and the computed position of Galileo were automated in a script that was executed by the telescope control computer. Thirty seconds prior to propagation, the script automatically pointed the telescope to the computed position of Galileo, and ten seconds after the end of the propagation, it repointed the telescope to the guide star. The position of the azimuth and elevation axes were recorded at the transmission time of each pulse.

F. Laser Diagnostics

The laser pulse width and energy were monitored by a Hamamatsu vacuum photodiode,² calibrated against a thermopile radiometer. Light to the vacuum photodiode consisted of the leakage through a turning mirror in the laser-beam injection optics. The thermopile radiometer was placed in the unattenuated beam. The output of the vacuum photodiode was digitized by a 1-GHz sample-rate digital oscilloscope at 1-nsec intervals and saved to a computer file. The pulse width was then computed from the digital data and the pulse energy was computed from the integral under the power-versus-time plot generated by the oscilloscope. The time of the trace was tagged to an accuracy of one millisecond by reading a WWV clock.

G. Communications and Data Transfer

Real-time communications between GOPEX control and SOR were via a dedicated phone line. A JPL representative was on-site to handle communications and monitor JPL control for permission to propagate, for unexpected

² Model number R1193U.

abort commands, and to report the status of each propagation to the GOPEX Task Manager. Backup communications consisted of telephones and fax machines over commercial phone lines.

Prior to operations and between experiment days, Galileo navigational data and position predictions were exchanged over the Internet between JPL and SOR computers. This computer network was also used to pass down-linked Galileo images from JPL to the SOR in near real time during operations.

H. Atmospheric Data

Separate instruments were used to monitor the atmospheric conditions during operations. The measurements made included Fried's coherence length, r_0 ; the isoplanatic angle, θ_0 ; and the atmospheric extinction using a lidar receiver to measure the strength of the atmospheric backscatter from each laser pulse. The coherence length and isoplanatic angle are measured by making modulation-transfer-function and scintillation measurements of light from a nearby bright star.

I. Data Recorded

The data recorded during the operations included

- (1) The time of the laser pulse to the nearest millisecond.
- (2) Instantaneous laser power versus time digitized in 1-nsec bins.
- (3) The telescope's azimuth position.
- (4) The telescope's elevation position.
- (5) The scan mirror's position off boresite.
- (6) The value of r_0 .
- (7) The value of θ_0 .
- (8) The lidar backscatter signal.

IV. Precursor Tests

Several propagation tests were conducted prior to operations with Galileo. SOR used Lageos and the Etalon artificial satellites and observed the retro-reflected signal return with a photomultiplier. The objectives of these tests were to (1) verify laser beam divergence and boresighting, (2) verify proper operation of the fast-steering mirror to scan the beam, and (3) get a rough idea of the beam profile.

On the mornings of October 1 and 2, 1992, successful laser uplink tests to Etalon 2 (Cosmos 2024) were conducted using 80- and 40- μ rad full-angle beam divergences. Returned signals were detected by a photomultiplier and outputs were saved on a digital oscilloscope. The photomultiplier was calibrated to allow an estimate of the number of photons detected. The beam was scanned across the satellite to measure beam divergence and boresighting and get a rough idea of the beam profile. The returned signal of the 40- μ rad beam was, on average, 3.6 (versus an expected value of 4) times stronger than the 80- μ rad beam. This represents a combined beam divergence discrepancy of 5 percent, well within the ± 10 -percent requirement set by JPL.

The scintillation of the return signal was quite severe, varying more than an order of magnitude. Average returns were approximately 400 detected photons for a 300-mJ laser pulse. The data-recording equipment did not permit collecting the hundreds or thousands of detections required to amass adequate statistics on beam-profile mapping. However, when the beam was moved in 10- μ rad steps from boresight, one could easily see a sudden drop in the return signal to an undetectable level at the predicted position at the edge of the beam. Signal return was nearly constant over a 30- to 40- μ rad radius for the 80- μ rad beam and dropped precipitously below 40 μ rad until it was completely undetectable at a 50- μ rad radius. A bias of approximately 20 μ rad was observed along the track of the satellite, which was consistent with the expected point-ahead angle.

On the morning of October 2, 1992, a 40- μ rad beam was propagated to Etalon 2. The telescope had to be pointed 23 μ rad ahead of the apparent position on the CCD camera. Without point-ahead correction, no detected signal was seen (consistent with a 40- μ rad full-angle beam divergence). By moving the telescope 20 μ rad off-center and observing a complete loss of signal, it was further verified that the beam was not more than 40 μ rad in diameter. Also, the fast-steering mirror was implemented in a 20- μ rad square pattern, which demonstrated the expected effect of scanning the beam. When the beam was centered on the satellite, no periodic time variation was seen in the return signal (mentally averaging the scintillation). When the beam was not centered on the satellite, one could see a definite cyclic temporal pattern in the return signal, which indicated that the satellite was being hit on only one position of the scan.

Additional precursor tests were performed on the morning and evening of October 26 using Lageos and Etalon at the 80- μ rad beam divergence. Return signal levels were

approximately a factor of 25 times stronger from Lageos than Etalon, as expected from the difference in range to the satellites. The beam was step-scanned again with the fast-steering mirror to demonstrate the desired effect.

A full dress rehearsal was conducted on the morning of November 18. All communications circuits and procedures were effected as planned for actual GOPEX operations. The SOR Test Director conducted operations according to a timeline-based checklist. No major problems were encountered, and the checklist was executed well ahead of schedule. The telescope script worked flawlessly, and with the exception of one 4- μ rad correction, telescope-pointing corrections were unnecessary. The timing and the scan mirror scripts worked flawlessly. Laser alignment held throughout the test to better than 0.5 μ rad. Atmospheric data were collected, and the weather was perfect. The dress rehearsal resulted in a few minor changes to the checklist and improvements in communications with JPL operations.

V. Galileo Operations

A. Overview

The biggest problem at the SOR during Galileo operations was the weather. Of the seven test nights, it was reasonably clear on only one night (the second night). The site was fogged in during the mornings of the last three experiment days, preventing any propagations. Fog is *not* the norm for Albuquerque, a city that experienced more precipitation in December 1992 than in any December in the previous 100 years! At times researchers were propagating through cloud cover so heavy that the guide star was not visible on the CCD camera. Furthermore, on the first experiment day, the relative humidity was so high that to prevent condensation, between propagations a hand-held heat gun had to be used to blow warm air on the secondary mirror of the telescope. In the worst conditions, snow was falling or fog was condensing into snow and falling into the open dome.

Despite the bad weather, SOR successfully conducted operations on the first four experiment days. Table 2 summarizes SOR pulses detected by Galileo. These data, from an article by B. M. Levine, K. S. Shaik, and T.-Y. Yan of JPL summarize the analysis of the GOPEX images [2]. No pulses were detected by Galileo from TMF or SOR for camera-shutter opening times less than 400 msec. Furthermore, there were always fewer pulse detections than possible for shutter times of 400, 533, and 800 msec. One explanation is that the scan motion of the camera on Galileo was not perfectly synchronized with the shutter opening.

B. Operations Procedures

Activities to prepare for, conduct, and assess the nightly operations were based on a test director's checklist and timeline designed to allow ample time to correct minor problems. Appendix A is a facsimile of the test director's checklist for day 344, the first test day.

In general, a test day involves facility preparation; equipment turn-on and warm-up; functional equipment checkout; computer disk-space and directory setup; optics and laser alignment; integrated system checkout; final preparations and double checks; conducting the experiment; postexperiment debriefing; data quick-look; and identification of problems to be fixed. Many of the details of these tasks can be gleaned from the timeline in Appendix A.

C. The First Test Day, December 9, 1992

Sixty propagation sequences were planned for the first test day. The first propagation was at 11:13:35 UTC and every three minutes thereafter until 14:12:32 UTC. Thirty pulses were transmitted during each sequence. On many of these sequences, the fast-steering mirror was stepped between pulses to generate one of the two patterns shown in Fig. 4.

Appendix B contains a sample of the summary of the propagation sequences, two graphs showing plots of each pulse in each propagation sequence of the measured pulse energies and pulse widths, and a sample output from a spreadsheet summarizing the laser diagnostic and telescope-pointing data for each pulse transmitted.

The propagation sequence summary that appears in Appendix B also lists the sequence number; the day number; the time of the first pulse, to the nearest millisecond; a propagation-time correction offset, if needed; the Galileo shutter time; the number of shots in a repeating sequence with no scan-mirror offset; the number of shots in a sequence at some offset radius; the radius size; and comments made during operations after each propagation sequence.

Appendix C contains plots of environmental conditions recorded at the site during Galileo operations. The weather was generally not good the first night. It had been cold (a few degrees above freezing) and rainy all day. After sunset, massive fog set in and in the early part of the evening the relative humidity was nearly 100 percent. It was not possible to open the facility for temperature conditioning, as scheduled, due to the high humidity. At around 08:30 UTC, the sky began to clear and the wind

picked up, blowing low-lying clouds to the southeast. However, the sky was too cloudy to permit using a star to set the focus of the telescope with the wavefront sensor. It was necessary to focus the telescope just before the first propagation, based on previous experience and the best image at the guide-star CCD camera. During the propagation sequences, the relative humidity averaged 82 percent. Between propagations, a person (standing atop a stepladder in the dark) directed warm air over the secondary with a hand-held heat gun in order to prevent condensation on the secondary mirror's surface. The temperature plot of the secondary mirror in Appendix C (the plot for temperature sensor TS037, December 9, 1992) shows this process. The data in Appendix C also show that the temperature in the pier (sensor TS030 at the source simulators) averaged a little over 13 deg C, while the outside temperature (sensor TS006) was approximately -1.5 deg C, a very large gradient indeed. These large temperature variations had an unknown, but certainly degrading, effect on the optical quality of the transmitted beam. It was not possible to make any r_0 or θ_0 measurements on the first night due to equipment malfunction.

B. M. Levine, of JPL's Optical Sciences and Applications Section, has analyzed the images from Galileo to determine which frames show detections and to measure their strength with respect to the background. He reports that Galileo detected pulses from SOR on propagation sequences 1, 13, 16, 17, 20, 28, and 32.³ Note from the comments in the propagation sequence table in Appendix B that the cloud cover was so thick that it was not possible to see the guide star between sequences 4 and 12. The scan mirror was on during sequences 16, 20, 28, and 32, and off during the other sequences. A summary appears in Table 3. The signal levels reported by JPL are included in this table. The average signal from TMF was data number (dn) 199.8, a value comparable to dn 173.8 from SOR. The high standard deviation (dn 212.2) of the signal variability could be due to the fact that most of the pulses were transmitted while the beam was being scanned.

D. The Second Test Day, December 10, 1992

This was the best test day at the SOR. The sky was nearly clear except for a very thin subvisible cirrus cloud layer at the 17.5-km range, which was present during the first 19 or 20 propagations. The relative humidity was still much higher than normal, averaging nearly 70 percent during the propagations. Generally, everything worked per-

³ B. M. Levine, private communication, Optical Sciences and Applications Section, Jet Propulsion Laboratory, Pasadena, California, December 22, 1992, updated by further private communication.

fectly on this night. Every pulse was transmitted, and atmospheric data were collected for every laser transmission.

Table 4 summarizes the pulse detections by Galileo. There were 37 detections with the average signal dn 143, a factor of more than three times higher than the average signal from TMF. The standard deviation was dn 187 and the maximum signal was dn 354. The laser energy was a bit higher, on average, for this day, and the sky was generally clear although not a "photometric night." The atmospheric seeing was not exceptional, in fact it was less than average for this site.

E. The Third Test Day, December 11, 1992

The weather was again a problem on the third night. The first 11 propagations were into very heavy clouds, and in most cases it was not possible to see the guide star. At propagation sequence number 12, the clouds thinned enough for a detection by Galileo. Detections were also made on sequences 16 and 20, which were the only other shutter openings of 533 msec. The very last propagation was into a fairly clear sky.

Table 5 summarizes the pulse detections for test day 3. Only 11 pulses from SOR were detected. The average signal level was dn 66.0 (compared with dn 54.5 from TMF). Five pulses were detected on the last sequence when the weather was clearest.

F. The Fourth Test Day, December 12, 1992

The cloud cover was variable on the fourth night. Only 10 propagation sequences were conducted. Only three of the sequences were 533 msec. The sky was clear on the first few propagations but became very cloudy after the sixth propagation.

Table 6 summarizes the detections by Galileo on frames 3 and 6. Only 5 pulses were detected. The average signal level was dn 33.6. No TMF data are available for comparison since the facility was weathered out completely on that night.

G. The Last Three Nights, December 14–16, 1992

There is nothing to report for these nights since SOR was completely fogged in on all three nights. The last recorded fog in December in Albuquerque occurred in 1937.

VI. Conclusions

GOPEX was a major success, with 268 pulse detections from TMF on six nights at 15 and 30 Hz, and 76 pulse detections from SOR on four nights at 10 Hz. The signal levels were close to those expected.

Acknowledgments

This experiment would not have been possible without the dedication and expertise of the SOR GOPEX Team. The team members and their areas of responsibility under the author's team leadership and test direction were C. Batcheller, aircraft spotter; B. Boeke, emission control and monitor engineer; R. Cleis, telescope pointing and monitor engineer; J. Drummond, lidar operation and data reduction; B. Ellerbroek, theoretical calculations; F. Gallegos, facility operator and weather monitor; J. Glover, scan mirror operator and countdown announcer; H. Hemmati, JPL representative; G. Jones, CCD guide-star camera operator; Joe Lange, propagation safety officer; P. Leatherman, lidar instrumentation; C. Morgenstern, atmospheric instrumentation; M. Oliker, data compilation and reduction; R. Ruane, laser equipment engineer; J. Spinhirne, optics design, setup, and alignment; P. Stech, Spectra Physics laser maintenance; D. Swindle, wavefront sensor operator and secondary mirror warmer; and S. Torney, aircraft spotter.

The team is also grateful to the programmatic support of Phillips Laboratory management, including John Anderson, SOR Division Chief; Bill Thompson, Ground-Based Laser Technology Program Manager; and Barry Hogge, Chief Scientist of the Lasers and Imaging Directorate. This project could not have been accomplished without their financial and managerial support. GOPEX Task Manager, Keith Wilson, and his supervisor, James R. Lesh, of the Optical Communications Group at JPL were instrumental in the success of the SOR Team.

References

- [1] K. E. Wilson and J. R. Lesh, "An Overview of the Galileo Optical Experiment (GOPEX)," *The Telecommunications and Data Acquisition Progress Report 42-114*, vol. April-June 1993, Jet Propulsion Laboratory, Pasadena, California, pp. 192-204, August 15, 1993.
- [2] B. M. Levine, K. S. Shaik, and T.-Y. Yan, "Data Analysis for GOPEX Image Frames," *The Telecommunications and Data Acquisition Progress Report 42-114*, vol. April-June 1993, Jet Propulsion Laboratory, Pasadena, California, pp. 213-229, August 15, 1993.

Table 1. GOPEX operations schedule.

Test day, December 1992	Start time, UTC	End time, UTC	Number of transmissions	Time between transmissions, min
9	11:13:35	14:12:32	60	3
10	11:06:21	13:04:38	40	3
11	11:10:06	12:07:44	20	3
12	10:25:24	11:19:59	10	6
14	10:42:08	11:37:45	12	5
15	10:39:54	11:25:24	10	5
16	10:39:41	11:15:04	8	5

Table 2. SOR pulses detected by Galileo.

Test day, day of year	Number of pulses detected
1, 344	16
2, 345	43
3, 346	12
4, 347	5
5, 349	No propagations due to fog
6, 350	No propagations due to fog
7, 351	No propagations due to fog

Table 3. Results for the first test day, day 344, December 9, 1992.

Propagation sequence	Sky condition	r_0 , cm	θ_0 , μ rad	Atmospheric transmission from lidar data	Average energy per pulse, mJ	Beam scan radius, μ rad	Galileo shutter time, msec	Number of pulses detected
1	Partly cloudy	No data	No data	0.77	310	0	400	1
13	Cloudy	No data	No data	0.92	312	0	400	2
16	Partly cloudy	No data	No data	0.81	312	60	800	4
17	Partly cloudy	No data	No data	0.80	315	0	400	2
20	Mostly cloudy	No data	No data	0.94	311	60	800	3
28	Good	No data	No data	0.80	315	30	400	1
32	Clear	No data	No data		317	30	400	1
Total number of detections		14						
Minimum dn		10						
Maximum dn		631						
Average dn		173.8						
Standard deviation dn		212.2						

Table 4. Results for the second test day, day 345, December 10, 1992.

Propagation sequence	Sky condition	r_0 , cm	θ_0 , μ rad	Atmospheric transmission from lidar data	Average energy per pulse, mJ	Beam scan radius, μ rad	Galileo shutter time, msec	Number of pulses detected
4	Subvisible cirrus	6.45	7.52	0.67	342	0	800	3
5	Subvisible cirrus	6.77	9.16	0.69	340	0	533	2
6	Subvisible cirrus	6.45	9.59	0.71	342	0	533	2
8	Subvisible cirrus	7.21	8.25	0.74	337	0	800	5
9	Subvisible cirrus	7.55	8.88	0.76	336	0	533	2
10	Subvisible cirrus	6.45	7.45	0.79	337	0	533	2
12	Subvisible cirrus	4.43	8.49	0.78	337	0	800	4
13	Subvisible cirrus	4.07	7.58	0.76	338	0	533	2
14	Subvisible cirrus	4.74	8.93	0.75	337	0	533	2
16	Subvisible cirrus	6.48	6.76	0.76	338	0	800	5
17	Subvisible cirrus	5.06	5.81	0.77	336	0	533	2
18	Subvisible cirrus	4.96	6.64	0.76	338	0	533	1
20	Clear	6.75	8.06	0.78	337	0	800	2
28	Clear	5.73	5.62	0.80	338	0	533	1
32	Clear	6.32	8.92	0.79	336	0	533	2
Total number of detections		37						
Minimum dn		14						
Maximum dn		354						
Average dn		143						
Standard deviation dn		187						

Table 5. Results for the third test day, day 346, December 11, 1992.

Propagation sequence	Sky condition	r_0 , cm	θ_0 , μrad	Atmospheric transmission from lidar data	Average energy per pulse, mJ	Beam scan radius, μrad	Galileo shutter time, msec	Number of pulses detected
12	Clouds	No data	No data	0.75	327	0	400	4
16	Very thick clouds	No data	No data	0.76	328	0	400	2
20	Fairly clear	9.18	4.67	0.75	327	60	800	5
Total number of detections		11						
Minimum dn		14						
Maximum dn		292						
Average dn		66						
Standard deviation dn		76						

Table 6. Results for the fourth test day, day 347, December 12, 1992.

Propagation sequence	Sky condition	r_0 , cm	θ_0 , μrad	Atmospheric transmission from lidar data	Average energy per pulse, mJ	Beam scan radius, μrad	Galileo shutter time, msec	Number of pulses detected
3	Clear	Est. 7.5	Est. 5.0	0.69	299	0	533	2
6	Very thick clouds	Est. 7.5	Est. 5.0	0.59	295	0	533	3
Total number of detections		5						
Minimum dn		6						
Maximum dn		81						
Average dn		33.6						
Standard deviation dn		30.1						

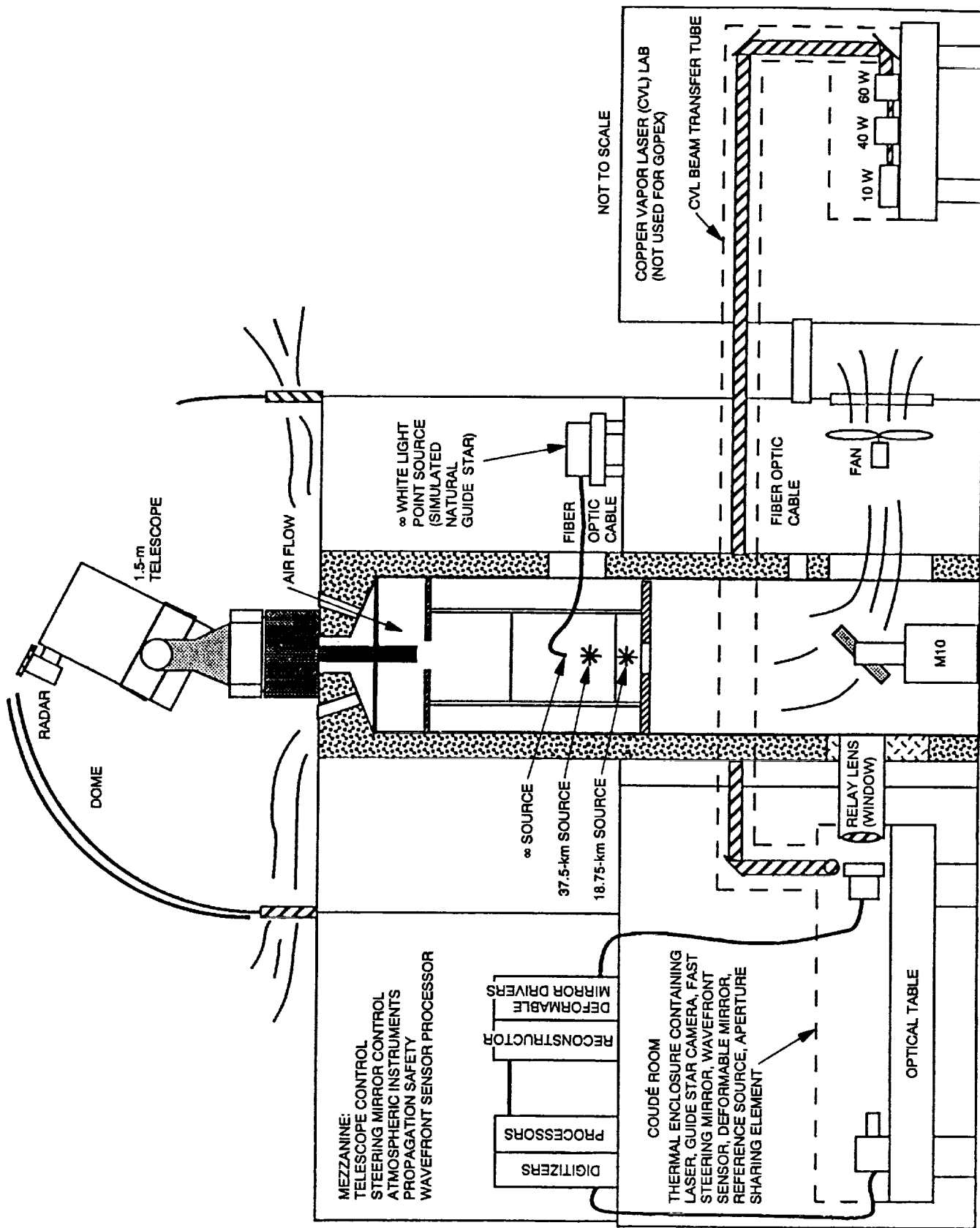


Fig. 1. Starfire Optical Range 1.5-m telescope facility.

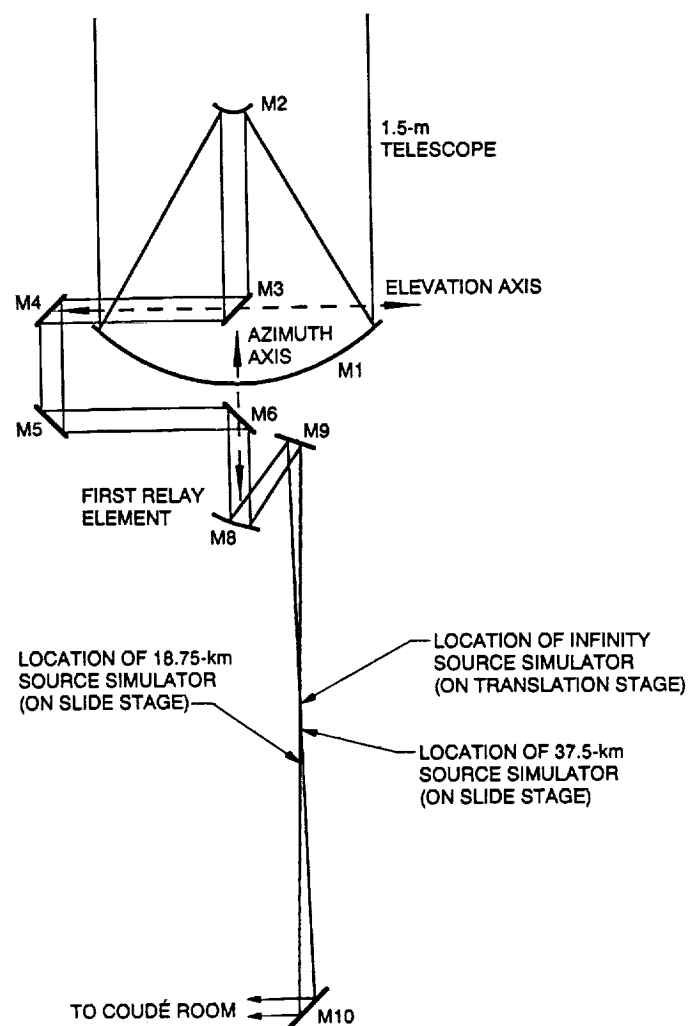


Fig. 2. Coudé path relay optics and source simulators for GOPEX.

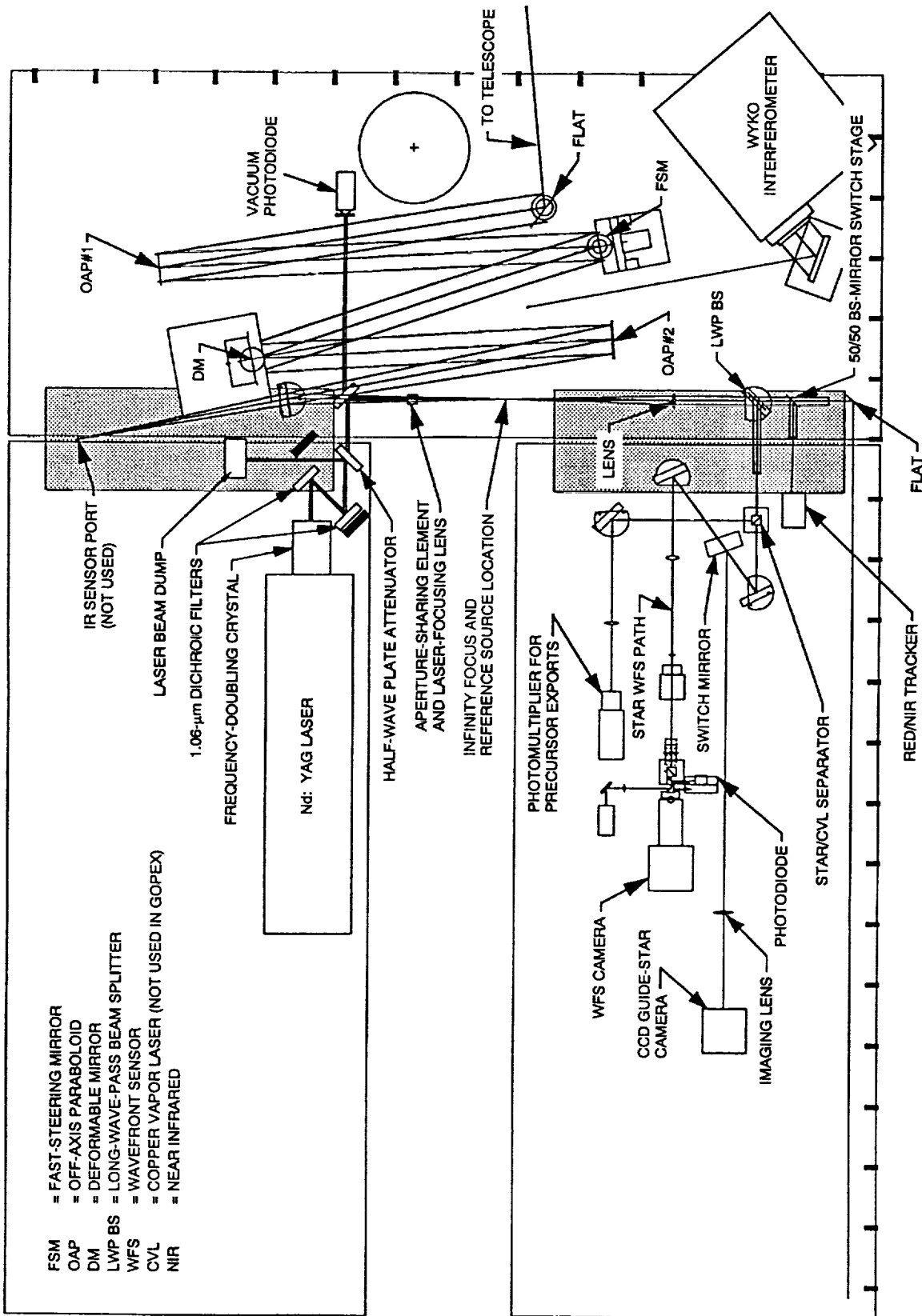


Fig. 3. Coude room optics layout at SOR, as configured for GOPEX.

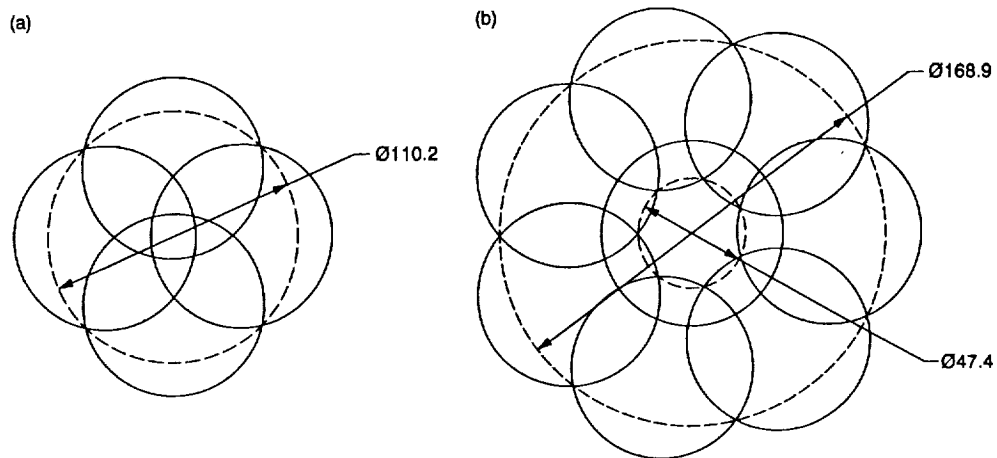


Fig. 4. GOPEX scan patterns used during the first test night, with an 80- μ rad beam divergence: (a) 4-pulse mode, no pulse on center, 30- μ rad offset and (b) 8-pulse mode, 1 pulse on center, 7 pulses at 60- μ rad offset.

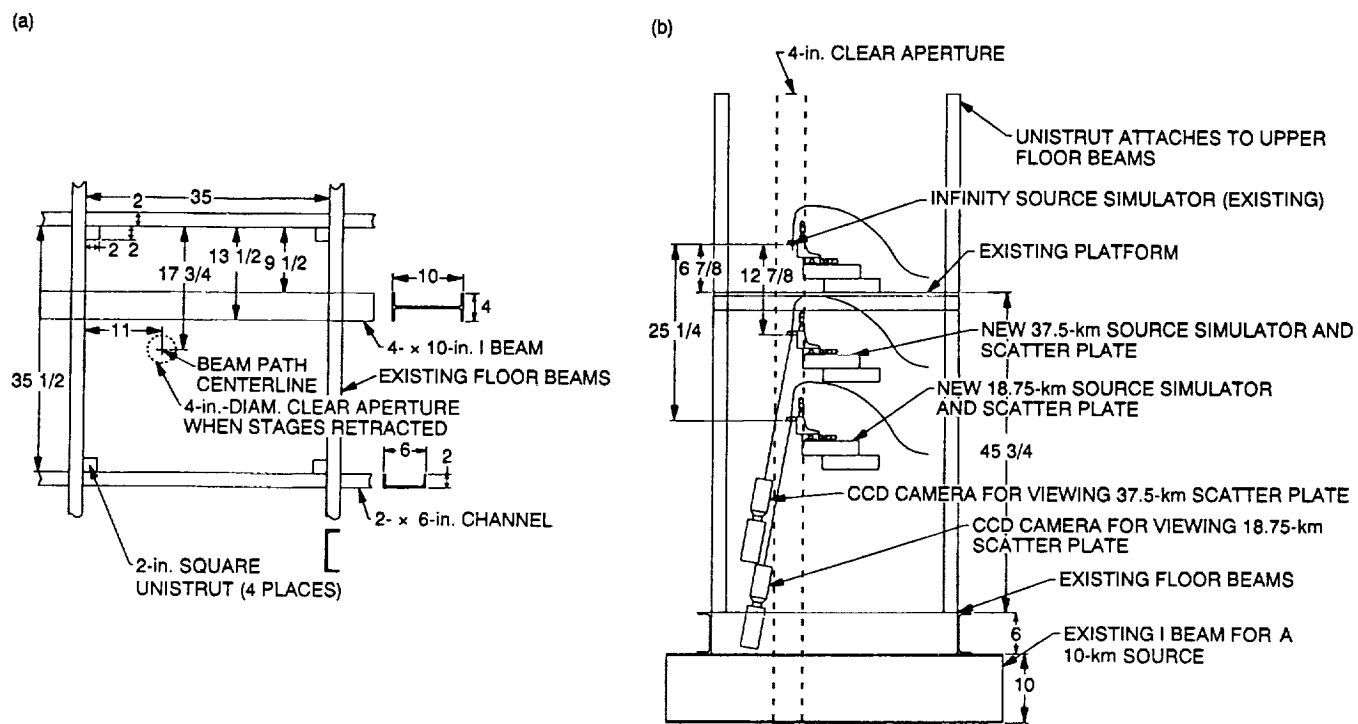


Fig. 5. 1.5-m pier area showing locations of new source simulators for GOPEX: (a) Top view and (b) side view.

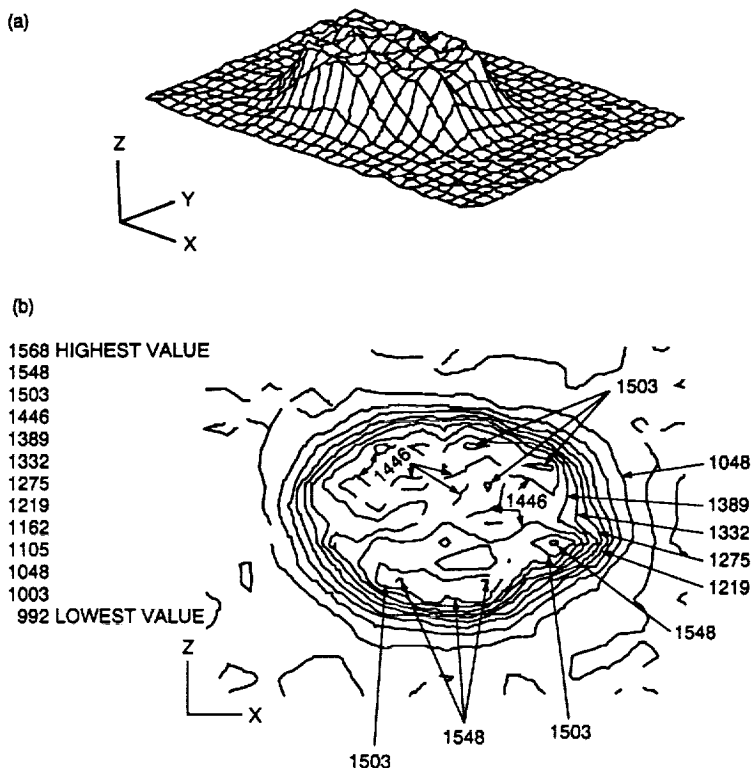


Fig. 6. Laser beam profile measured 127 cm in front of the laser. The beam is round, the distortion is due to the printer: (a) 3-D profile and (b) contour plot.

Appendix A

Test Director's Checklist

An example of the test director's checklist is shown on the following pages.

GOPEX at SOR						
Test Director's Check List						
Assigned Facility Operator (FO)	Fred Gallegos					
Test Day	344					
Beam Divergence	80					
First Propagation	11:13:34					
Test Director	✓ Bob Fugate					
JPL Representative	✓ Hamid Hemmati					
Facility operator	Fred Gallegos					
Spotter 1	✓ Curt Batcheller					
Spotter 2	✓ Steve Torney					
Safety Officer	✓ Joe Lange					
Telescope Operator	✓ Rick Cleis					
Lidar Operator	✓ Phil Leatherman	Jack Drummond.				
r0 Operator	✓ Carolyn Morgenstern	Mike Brady				
Wavefront Sensor Operator	✓ Dave Swindle					
Photometrics Operator	✓ Gary Jones					
Optics and Laser Operator	✓ Jim Spinheimer					
Laser Diagnostics Operator	✓ Bruce Boete					
Laser Maintenance	✓ Paul Steck					
Data Reduction	✓ Mike Oliker					
Task	T-time	Scheduled Start time (UTC)	To be completed by (init)	Completed by (initiate)	Actual Completion Time	Comments
FACILITY PREPARATION						
Open domes	8:00	3:13	FO			
Open dome shutters	7:45	3:28	FO			
Uncover 1.5 m tele	7:40	3:33	FO			
Uncover r0 tele	7:35	3:38	FO			
Turn on pier fan	7:30	3:43	FO			
Record site temps	7:25	3:48	FO	RDF	03:50	
Record wind data	7:20	3:53	FO	RDF	03:50	
Record RH data	7:15	3:58	FO	RDF	03:50	
Check all sky camera	7:10	4:03	FO	RDF	03:55	
Turn on WEFAx	7:05	4:08	FO	RDF	02:30	
Turn on telescope control computer	7:30	3:43	WJL	RDF	04:15	Turn on early for pics/prognosis
Turn on 1.5 m tele control console	7:20	3:53	WJL	RDF	05:20	Delayed
Turn on safety officer's console	7:10	4:03	WJL		04:15	Delayed
Turn on aircraft detection radar	7:05	4:08	WJL			Delayed
Perform radar check	7:00	4:13	WJL			Delayed.
Pre-test Briefing	6:30	4:43	RCF	RDF	05:20	Bruce Boete absent
EQUIPMENT TURN-ON						
Spotter comm and kill switch	6:00	5:13	TEAM			
r0 telescope and control computer	6:00	5:13	CB	WJL	05:21	
r0 Instrumentation computer	6:00	5:13	CM			
LIDAR receiver electronics	5:50	5:23	CM			
Annotation computer	6:00	5:13	PL	PL	05:25	
Wavefront sensor camera and cooler	6:00	5:13	RAC			already on
Wavefront sensor control computer	5:55	5:18	MDO	DWS	05:28	
Real time digital reconstructor	5:50	5:23	MDO	DWS	05:30	
Digital reconstructor control computer	5:45	5:28	MDO	DWS	05:32	
Digital reconstructor diagnostic computers	5:38	5:35	MDO	DWS	05:35	
Photometrics camera and cooler	6:00	5:13	GJ	GJ	05:25	
Photometrics control computer	5:50	5:23	GJ	GJ	05:26	
Tilt mirror power supply and electronics	5:40	5:33	RAC	RAC	05:20	
Timing and tilt mirror control computer	5:35	5:38	RAC	RAC	05:22	
Tracker electronics	5:28	5:45	RAC	RAC	05:22	
Vacuum photodiode high voltage power supp	6:00	5:13	BRB	BRB	05:40	
Digital oscilloscope for pulse monitoring	6:55	5:18	BRB	BRB	05:40	
Laser diagnostics computer	5:50	5:23	BRB	BRB	05:40	
Laser water chiller and heat exchanger	6:00	5:13	RER	RER	05:50	
Laser power supply and control electronics	6:50	5:23	RER	RER	05:50	
FUNCTIONAL EQUIPMENT CHECK						
CB (spotter equipment)	5:30	5:43	RCF	RDF	05:45	
WJL (all safety equipment)	6:28	5:45	RCF	RDF	05:40	
CM (r0 instrumentation)	5:26	5:47	RCF	RDF	X	
PL (LIDAR electronics)	5:25	5:48	RCF	RDF	X	Delayed due to wx - A/D Failure
MDO (wavefront sensor and reconstructor)	5:24	5:49	RCF	DWS	05:40	Delayed " " " -- No precheck testable
GJ (photometric camera)	5:22	5:51	RCF	RDF	06:00	
BRB (laser diagnostic equipment)	5:20	5:53	RCF	RDF	06:15	
RAC (telescope and control electronics)	6:16	5:58	RCF	RDF	05:50	
RAC (tilt mirror and laser timing)	5:10	6:03	RCF	RDF	05:20	
RER (laser and cooling equipment)	5:05	6:08	RCF	RDF	06:10	
FO (met equipment)	5:03	6:10	RCF	RDF	06:09	
Load pointing files	5:00	6:13	RCF	RDF	02:10	

Fig. A-1. Test director's checklist for GOPEX, day 344, December 9, 1992.

Fig. A-1. (contd)

Appendix B

Day 344, December 9, 1992

This section contains summaries of the Galileo operations activities for day 344, the first test day.

	A	B	C	D	E	F	G	H	I	J	K	L
8							prop	GLL				
9							time	shutter	#center	#radius	radius	Comments
7 seq	number	day	hr	min	sec	ms	correct	time	shots	shots	size	
8												
9												
10												
11 001	344	11	13	35	284	0	400	4	0	0	Partly cloudy	
12 002	344	11	18	37	259	0	400	0	4	30	No transmission	
13 003	344	11	19	39	164	0	200	2	0	0	cloudy	
14 004	344	11	22	41	449	0	800	1	7	60	Very cloudy - super dense, cannot see the guide star	
15 005	344	11	25	43	242	0	400	4	0	0	same	
16 006	344	11	29	45	237	0	400	0	4	30	same	
17 007	344	11	31	47	131	0	200	2	0	0	same	
18 008	344	11	34	49	426	0	800	1	7	60	same	
19 009	344	11	37	51	221	0	400	4	0	0	same	
20 010	344	11	40	53	215	0	400	0	4	30	same	
21 011	344	11	43	55	110	0	200	2	0	0	same	
22 012	344	11	48	57	405	0	800	1	7	60	same	
23 013	344	11	49	59	200	0	400	4	0	0	cloudy	
24 014	344	11	53	01	193	0	400	0	4	30	clearing	
25 015	344	11	56	03	088	0	200	2	0	0	clearing	
26 016	344	11	59	05	382	0	800	1	7	60	partly cloudy - but aborted part way through	
27 017	344	12	02	07	177	0	400	4	0	0	partly cloudy	
28 018	344	12	05	09	172	0	400	0	4	30	good	
29 019	344	12	08	11	087	0	200	2	0	0	partly cloudy	
30 020	344	12	11	13	361	0	800	1	7	60	mostly cloudy	
31 021	344	12	14	15	056	0	200	2	0	0	mostly cloudy, can see the guide star	
32 022	344	12	17	17	050	0	200	2	0	0	partly cloudy	
33 023	344	12	20	19	011	0	133	1	0	0	partly cloudy	
34 024	344	12	23	21	138	0	400	0	4	30	partly cloudy	
35 025	344	12	26	23	033	0	200	2	0	0	partly cloudy	
36 026	344	12	29	25	028	0	200	2	0	0	good	
37 027	344	12	32	28	969	0	133	1	0	0	good	
38 028	344	12	35	29	117	0	400	0	4	30	good	
39 029	344	12	38	31	012	0	200	2	0	0	good	
40 030	344	12	41	33	007	0	200	2	0	0	good	
41 031	344	12	44	34	966	0	133	1	0	0	cloudy - no guide star	
42 032	344	12	47	37	095	0	400	0	4	30	clear	
43 033	344	12	50	38	990	0	200	2	0	0	partly cloudy	
44 034	344	12	53	40	984	0	200	2	0	0	clear	
	A	B	C	D	E	F	G	H	I	J	K	L
45 035	344	12	56	42	945	0	133	1	0	0	partly cloudy	
46 036	344	12	59	45	074	0	400	0	4	30	partly cloudy - beam was on late	
47 037	344	13	02	46	987	0	200	2	0	0	no transmission due to technical difficulties	
48 038	344	13	05	48	982	0	200	2	0	0	partly cloudy	
49 039	344	13	08	50	924	0	133	1	0	0	partly cloudy	
50 040	344	13	11	53	050	0	400	0	4	30	partly cloudy	
51 041	344	13	14	54	945	0	200	2	0	0	very cloudy	
52 042	344	13	17	56	940	0	200	2	0	0	very cloudy	
53 043	344	13	20	58	901	0	133	1	0	0	very cloudy	
54 044	344	13	24	01	029	0	400	0	4	30	very cloudy	
55 045	344	13	27	02	923	0	200	2	0	0	semi clear	
56 046	344	13	30	04	918	0	200	2	0	0	clear - stopped scanning starting with this sequence	
57 047	344	13	33	06	879	0	133	1	0	0	semi clear	
58 048	344	13	36	09	006	0	400	0	4	30	clearing	
59 049	344	13	39	10	001	0	200	2	0	0	clearing but getting very light - think lessing delayed by 2 seconds not 1 sec asked for	
60 050	344	13	42	12	886	0	200	2	0	0	clearing - propagation two seconds later than time at left	
61 051	344	13	45	14	856	0	133	1	0	0	clearing - propagation 1 sec later than time at left	
62 052	344	13	48	16	984	0	400	0	4	30	clear - all propagations from here on are one second later than published times at left	
63 053	344	13	51	16	879	0	200	2	0	0	clear	
64 054	344	13	54	20	873	0	200	2	0	0	clear	
65 055	344	13	57	22	835	0	133	1	0	0	clear	
66 056	344	14	00	24	962	0	400	0	4	30	clear	
67 057	344	14	03	26	858	0	200	2	0	0	clear	
68 058	344	14	06	28	851	0	200	2	0	0	clear	
69 059	344	14	09	30	812	0	133	1	0	0	clear	
70 060	344	14	12	32	940	0	400	0	4	30	clear	

Fig. B-1. Propagation sequences for GOPEX, day 344, December 9, 1992.

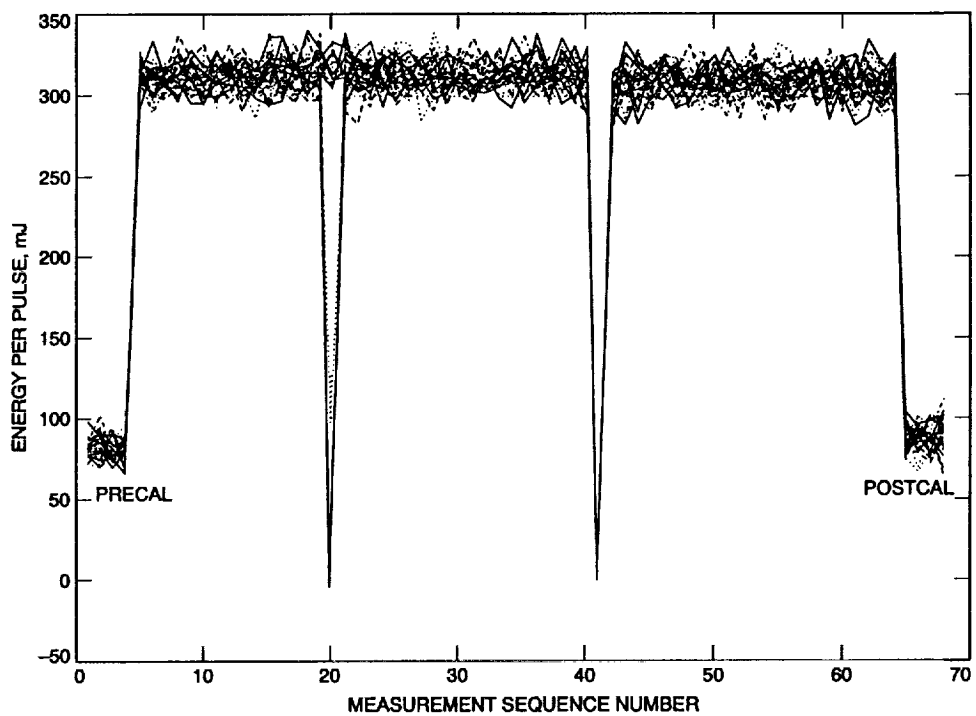


Fig. B-2. Plot of measured energy per pulse for each propagation sequence and for precalibration and postcalibration runs at lower power. The graph contains 30 points for each propagation sequence, corresponding to the 30 pulses propagated during each sequence. The atmospheric transmission sequences start at sequence number 5 and end at number 65. The drop-outs at number 20 and at number 41 were caused by laser Q-switch problems.

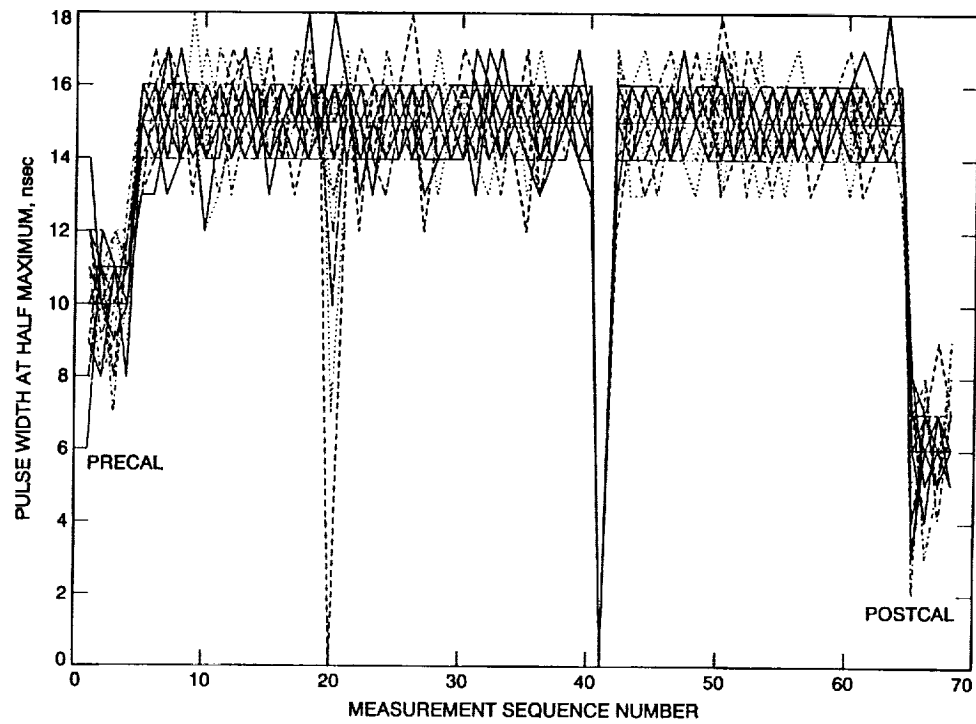


Fig. B-3. Plot of measured full-width half-maximum laser pulse widths for each of the atmospheric propagation sequences (numbers 5 through 65) and during pre- and postcalibration of the laser calorimeter (numbers 1–5 and 65–68). Thirty measurements (corresponding to 30 pulses) are plotted for each propagation sequence.

Seq	Day	Hrs	Mins	Secs	msecs	Act. Pmt	TIME	GOPEX		READ		READ		ERROR		GOAL		GOAL		OFFSET		EL AN ABER		REFRACT		IMPROV						
								msecs	Num	days	mJ	ns	degrees	degrees	rad	rad	degrees	degrees	rad	rad	rad	rad	rad	rad	rad	rad	X Pos	Y Pos				
1	344	11	13	35	261	-2.0		1	344.4677769236111	313	13	228.0409	38.0523	-2.1	-0.2	175.1628	-5.7345	80.0	26.6	0.0	0.0	287.9	0	0	0	0	0	0	0	0	0	
								2	344.46777039518	322	16	228.0419	38.0530	0.9	3.3	175.1628	-5.7345	80.0	26.6	0.0	0.0	287.9	0	0	0	0	0	0	0	0	0	0
								3	344.467771550925	310	16	228.0419	38.0530	0.9	3.3	175.1628	-5.7345	80.0	26.6	0.0	0.0	287.9	0	0	0	0	0	0	0	0	0	0
								4	344.467772708333	319	14	228.0428	38.0532	0.6	-0.8	175.1628	-5.7345	80.0	26.6	0.0	0.0	287.9	0	0	0	0	0	0	0	0	0	0
								5	344.467775023148	307	13	228.0436	38.0540	0.0	4.5	175.1628	-5.7345	80.0	26.6	0.0	0.0	287.9	0	0	0	0	0	0	0	0	0	0
								7	344.467776180555	320	16	228.0436	38.0540	0.0	4.5	175.1628	-5.7345	80.0	26.6	0.0	0.0	287.9	0	0	0	0	0	0	0	0	0	0
								8	344.467777337962	309	16	228.0444	38.0543	-0.2	1.0	175.1628	-5.7345	80.0	26.6	0.0	0.0	287.8	0	0	0	0	0	0	0	0	0	0
								9	344.467778495370	307	15	228.0444	38.0543	-0.2	1.0	175.1628	-5.7345	80.0	26.6	0.0	0.0	287.8	0	0	0	0	0	0	0	0	0	0
								10	344.4677795652777	322	16	228.0453	38.0548	1.0	0.1	175.1628	-5.7345	80.0	26.6	0.0	0.0	287.8	0	0	0	0	0	0	0	0	0	0
								11	344.467780810185	306	16	228.0453	38.0548	1.0	0.1	175.1628	-5.7345	80.0	26.6	0.0	0.0	287.8	0	0	0	0	0	0	0	0	0	0
								12	344.4677819675928	309	16	228.0462	38.0552	0.4	-0.9	175.1627	-5.7345	80.0	26.6	0.0	0.0	287.8	0	0	0	0	0	0	0	0	0	0
								13	344.467783124099	306	15	228.0462	38.0552	0.4	-0.9	175.1627	-5.7345	80.0	26.6	0.0	0.0	287.8	0	0	0	0	0	0	0	0	0	0
								14	344.467784282407	309	14	228.0471	38.0556	1.6	1.2	175.1627	-5.7345	80.0	26.6	0.0	0.0	287.8	0	0	0	0	0	0	0	0	0	0
								15	344.467785439814	302	15	228.0471	38.0556	1.6	1.2	175.1627	-5.7345	80.0	26.6	0.0	0.0	287.8	0	0	0	0	0	0	0	0	0	0
								16	344.467786597222	326	14	228.0479	38.0563	0.7	-0.1	175.1627	-5.7345	80.0	26.6	0.0	0.0	287.8	0	0	0	0	0	0	0	0	0	0
								17	344.467787754629	312	15	228.0479	38.0563	0.7	-0.1	175.1627	-5.7345	80.0	26.6	0.0	0.0	287.8	0	0	0	0	0	0	0	0	0	0
								18	344.467788012037	308	16	228.0486	38.0566	-0.9	-2.1	175.1627	-5.7345	80.0	26.6	0.0	0.0	287.8	0	0	0	0	0	0	0	0	0	0
								19	344.467789069444	308	15	228.0486	38.0566	-0.9	-2.1	175.1627	-5.7345	80.0	26.6	0.0	0.0	287.8	0	0	0	0	0	0	0	0	0	0
								20	344.467791226851	320	16	228.0495	38.0572	-0.8	-0.7	175.1627	-5.7345	80.0	26.6	0.0	0.0	287.8	0	0	0	0	0	0	0	0	0	0
								21	344.467792364250	310	15	228.0495	38.0572	-0.8	-0.7	175.1627	-5.7345	80.0	26.6	0.0	0.0	287.8	0	0	0	0	0	0	0	0	0	0
								22	344.467792364166	310	15	228.0504	38.0576	-0.7	-0.1	175.1627	-5.7345	80.0	26.6	0.0	0.0	287.8	0	0	0	0	0	0	0	0	0	0
								23	344.467794690074	312	16	228.0504	38.0576	-0.7	-0.1	175.1627	-5.7345	80.0	26.6	0.0	0.0	287.8	0	0	0	0	0	0	0	0	0	0
								24	344.467795856481	312	15	228.0513	38.0583	0.9	1.5	175.1627	-5.7345	80.0	26.6	0.0	0.0	287.8	0	0	0	0	0	0	0	0	0	0
								25	344.467797013088	317	16	228.0513	38.0583	0.9	1.5	175.1627	-5.7345	80.0	26.6	0.0	0.0	287.8	0	0	0	0	0	0	0	0	0	0
								26	344.467798171298	308	15	228.0521	38.0587	0.3	-0.2	175.1627	-5.7345	80.0	26.6	0.0	0.0	287.8	0	0	0	0	0	0	0	0	0	0
								27	344.467799328703	302	14	228.0521	38.0587	0.3	-0.2	175.1627	-5.7345	80.0	26.6	0.0	0.0	287.8	0	0	0	0	0	0	0	0	0	0
								28	344.467800486111	319	15	228.0529	38.0592	-1.3	-0.1	175.1627	-5.7345	80.0	26.6	0.0	0.0	287.8	0	0	0	0	0	0	0	0	0	0
								29	344.467801643518	291	16	228.0529	38.0592	-1.3	-0.1	175.1627	-5.7345	80.0	26.6	0.0	0.0	287.8	0	0	0	0	0	0	0	0	0	0
								30	344.467802800925	318	13	228.0536	38.0597	-0.5	-0.4	175.1627	-5.7345	80.0	26.6	0.0	0.0	287.8	0	0	0	0	0	0	0	0	0	0
	2	344	11	16	37	257	-1.0	1	344.469075671206	333	13	228.0523	38.5027	-0.6	0.3	175.1554	-5.7325	80.0	26.6	0.0	0.0	283.2	0	0	0	0	0	0	0	0	0	0
								2	344.469076828703	313	16	228.0524	38.5032	-0.8	1.2	175.1554	-5.7325	80.0	26.6	0.0	0.0	283.2	0	0	0	0	0	0	0	0	0	0
								3	344.469077986111	318	15	228.0524	38.5032	-0.8	1.2	175.1554	-5.7325	80.0	26.6	0.0	0.0	283.2	0	0	0	0	0	0	0	0	0	0
								4	344.469079143518	308	14	228.0525	38.5035	-0.6	-3.5	175.1554	-5.7325	80.0	26.6	0.0	0.0	283.2	0	0	0	0	0	0	0	0	0	0
								5	344.46908030925	311	16	228.0525	38.5035	-0.6	-3.5	175.1554	-5.7325	80.0	26.6	0.0	0.0	283.2	0	0	0	0	0	0	0	0	0	0
								6	344.469081458333	317	16	228.0527	38.5041	-2.5	-1.6	175.1554	-5.7325	80.0	26.6	0.0	0.0	283.2	0	0	0	0	0	0	0	0	0	0
								7	344.469082815740	322	15	228.0527	38.5041	-2.5	-1.6	175.1554	-5.7325	80.0	26.6	0.0	0.0	283.2	0	0	0	0	0	0	0	0	0	0
								8	344.469083773148	309	16	228.0527	38.5047	-0.3	0.3	175.1554	-5.7325	80.0	26.6	0.0	0.0	283.2	0	0	0	0	0	0	0	0	0	0
								9	344.469084030559	315	15	228.0527	38.5047	-0.3	0.3	175.1554	-5.7325	80.0	26.6	0.0	0.0	283.2	0	0	0	0	0	0	0	0	0	0
								10	344.469086087962	319	16	228.0527	38.5052	-1.4	1.7	175.1554	-5.7325	80.0	26.6	0.0	0.0	283.2	0	0	0	0	0	0	0	0	0	0
								11	344.469088245370	293	15	228.0527	38.5052	-1.4	1.7	175.1554	-5.7325	80.0	26.6	0.0	0.0	283.2	0	0	0	0	0	0	0	0	0	0

Fig. B-4. First-night results for GOPEX, day 344, December 9, 1992.

Appendix C

Sample of environmental data collected during transmissions.

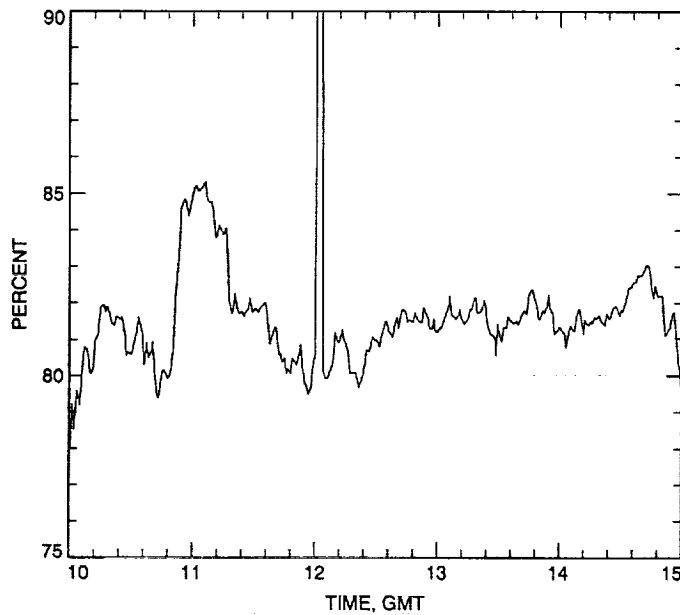


Fig. C-1. Computed relative humidity, day 344, December 9, 1992.

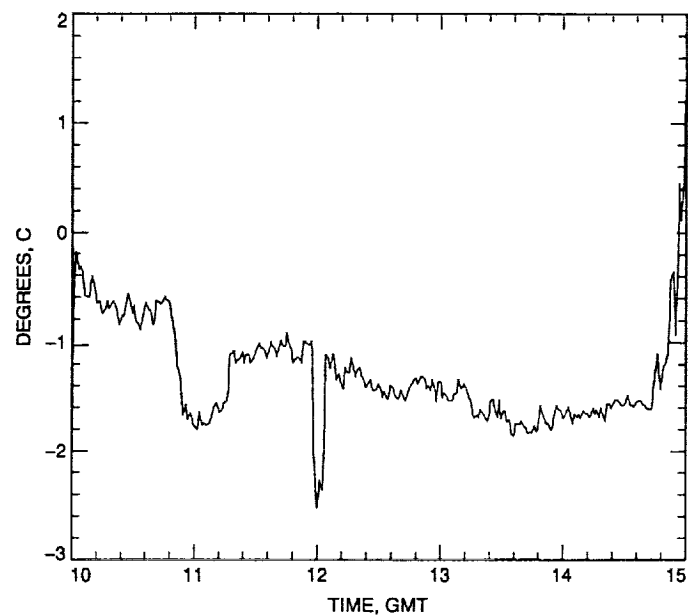


Fig. C-3. Ambient air temperature, Tower Number 1, day 344, December 9, 1992.

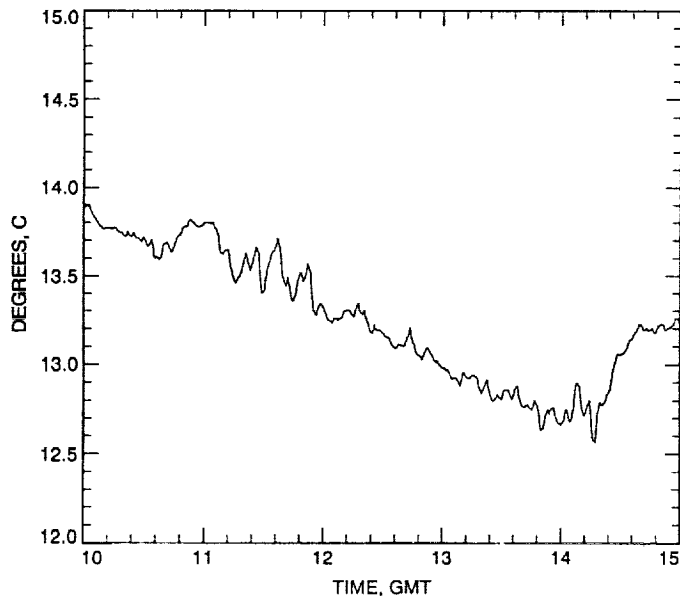


Fig. C-2. Optical path air temperature at the (source simulator) (see Fig. 2), day 344, December 9, 1992.

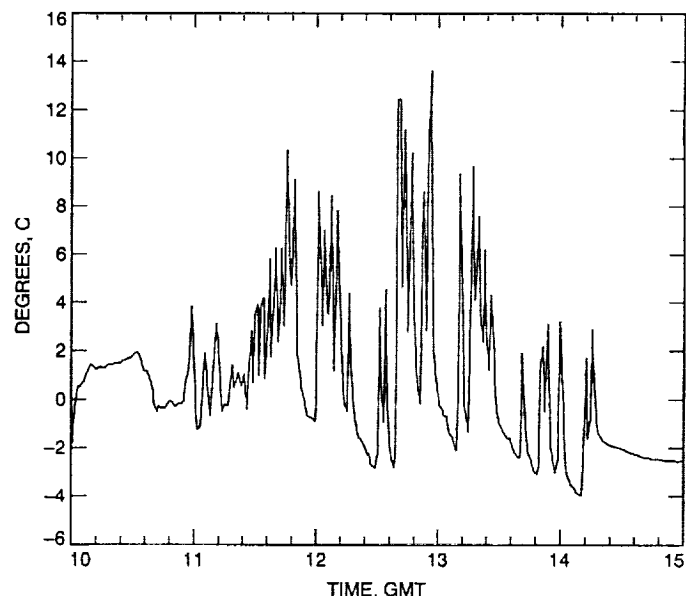


Fig. C-4. Secondary mirror temperature, day 344, December 9, 1992.

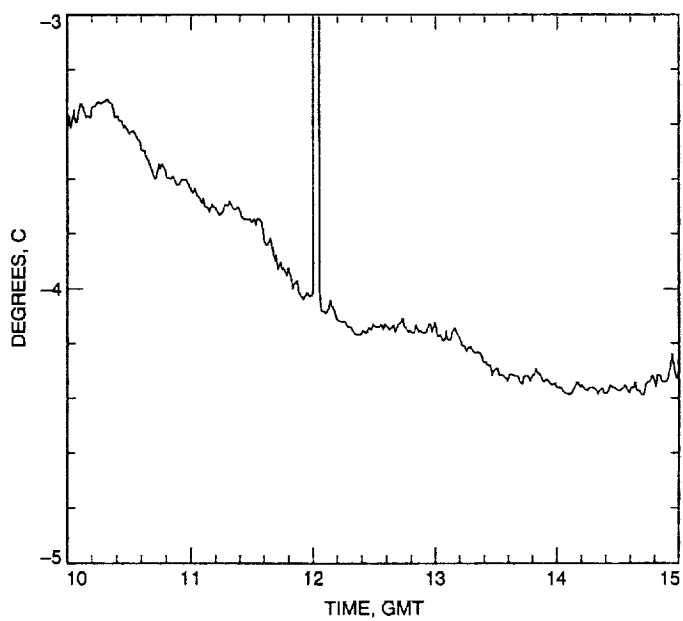


Fig. C-5. Ambient air dew point, Tower Number 2, day 344,
December 9, 1992.

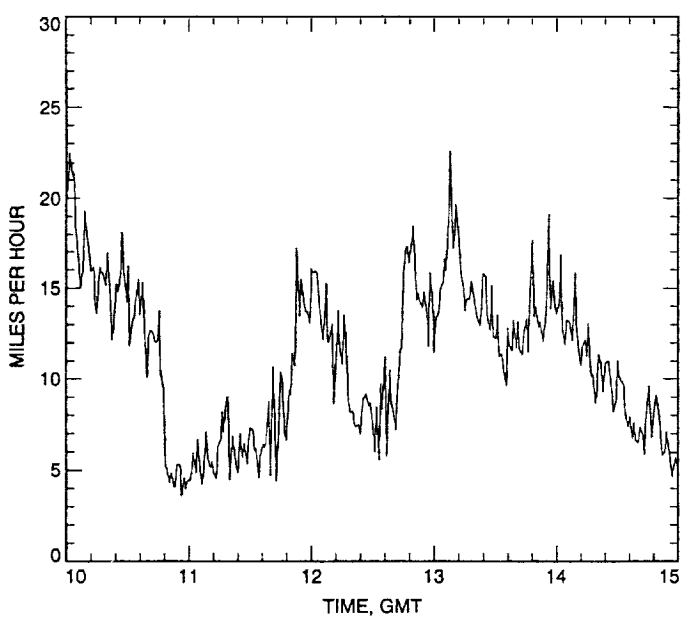


Fig. C-6. Tower Number 1 wind speed, top, day 344, December 9,
1992.

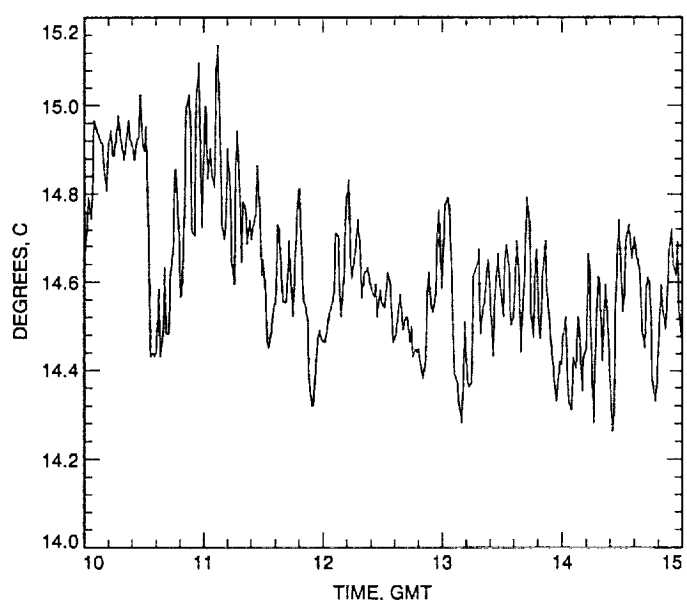


Fig. C-7. Optical path air temperature at M8 (see Fig. 2), day 344,
December 9, 1992.